



UNIVERSITY OF LEEDS

This is a repository copy of *The incorporation of nanoscale particles to enhance the properties of oriented polymers*.

White Rose Research Online URL for this paper:  
<http://eprints.whiterose.ac.uk/95624/>

Version: Accepted Version

---

**Proceedings Paper:**

Foster, RJ, Hine, PJ and Ward, IM (2006) The incorporation of nanoscale particles to enhance the properties of oriented polymers. In: UNSPECIFIED European Conference on Composite Materials 12, 29 Aug 2006 - 01 Sep 2005, Biarritz, France. . (Unpublished)

---

**Reuse**

Unless indicated otherwise, fulltext items are protected by copyright with all rights reserved. The copyright exception in section 29 of the Copyright, Designs and Patents Act 1988 allows the making of a single copy solely for the purpose of non-commercial research or private study within the limits of fair dealing. The publisher or other rights-holder may allow further reproduction and re-use of this version - refer to the White Rose Research Online record for this item. Where records identify the publisher as the copyright holder, users can verify any specific terms of use on the publisher's website.

**Takedown**

If you consider content in White Rose Research Online to be in breach of UK law, please notify us by emailing [eprints@whiterose.ac.uk](mailto:eprints@whiterose.ac.uk) including the URL of the record and the reason for the withdrawal request.



[eprints@whiterose.ac.uk](mailto:eprints@whiterose.ac.uk)  
<https://eprints.whiterose.ac.uk/>

# THE INCORPORATION OF NANOSCALE PARTICLES TO ENHANCE THE PROPERTIES OF ORIENTED POLYMERS

R. J. Foster<sup>1</sup>, P. J. Hine<sup>2</sup> and I. M. Ward<sup>3</sup>

IRC in Polymer Science and Technology  
Polymer and Complex Fluids Group  
School of Physics and Astronomy  
University of Leeds, Leeds, UK  
LS2 9JT

[1phyrjf@phys-irc.leeds.ac.uk](mailto:phyrjf@phys-irc.leeds.ac.uk), [2p.j.hine@leeds.ac.uk](mailto:p.j.hine@leeds.ac.uk), [3i.m.ward@leeds.ac.uk](mailto:i.m.ward@leeds.ac.uk)

## ABSTRACT

The incorporation of nanoscale particles into oriented polymers offers the potential to enhance the properties of the resultant nanocomposites. Vapour-grown carbon nanofibres (CNF) are particularly favoured due to high particle shape anisotropy (~10-100), high modulus (240GPa), and are readily available. CNF have been incorporated into polypropylene (PP) using a twin-screw extruder, and the nano-filled material has then been oriented by melt-spinning and solid phase drawing, to produce high modulus, highly oriented tapes, that are then formed into thick section homogeneous sheets, using the hot compaction process developed at the University of Leeds. Preliminary static tensile testing results of uniaxially wound hot compacted samples show an increase in the Young's modulus from 6.6GPa to 8.5GPa, at the optimum compaction conditions, over unfilled hot compacted PP. Results of varying the blending and compaction conditions are reported, along with investigation into the length, orientation and dispersion of the CNF in the PP matrix, using a variety of techniques including dynamic light scattering (DLS) and scanning electron microscopy (SEM).

## 1. Introduction

Hot compaction utilises high modulus, highly oriented elements to form thick section homogeneous sheets without the need to introduce a second phase of different chemical composition, for example an epoxy resin. These 'single polymer' composites are produced by selectively melting the surface of the oriented elements, which on cooling epitaxially crystallise onto the backbone of the oriented elements to form a matrix phase, binding the structure together.

The process of hot compaction is applicable to a wide range of thermoplastic materials. Initially various grades of polyethylene fibres and tapes were successfully compacted [1, 2]. It was, however, polypropylene that showed the greatest potential as a commercial product [3]. Although hot compacted polypropylene shows improved mechanical properties, in particular Young's modulus, over isotropic polypropylene sheet [4, 5], the improvement is not sufficient for some potential areas of commercial exploitation, especially in the automotive industry at elevated temperatures.

Interest into nanoscale particles as particulate fillers in polymer composites is an active research area worldwide and a number of nanoparticle filled thermoplastic composites, including polypropylene-carbon nanofibre composites, have been reported [6-9]. Unfilled polymer materials, including hot compacted thermoplastic polymers proved successful commercially due to the combination of being lightweight, low cost, and easy to process. Nanoscale fillers offer the potential of reinforcement of these materials without detracting from the advantages of working with polymers.

Initial research incorporating vapour-grown carbon nanofibres (CNF) into polypropylene to produce a hot compacted composite, has shown promising results [10], although it has become clear that a more in-depth characterisation of the composite and properties is necessary. Of particular interest is a determination of the optimum conditions for processing and hot compaction in order to take the material through to possible commercial

use, and to link the structure of the material to its properties through modelling. Preliminary results of this investigation are presented here.

## 2. Experimental Results and Discussion

### 2.1 Blending of Vapour-Grown Carbon Fibres with Polypropylene

CNF purchased from Applied Sciences Inc, Cedarville, Ohio, USA (Pyrograf III™, type PR-19, grade PS) were blended with BP grade 100GA02 polypropylene pellets using a twin-screw extruder, at a loading of 10% w/w CNF. The effect of blending temperature on the properties of the composite was investigated by setting the extruder's barrel temperature profile, such that all heating zones were set to either 200 or 230°C. The screw speed was set to ~70rpm.

The twin-screw extruder was set up so that there were three mixing zones along the length barrel of the extruder. Polypropylene pellets were fed into the extruder at the beginning of the screw, and the CNFs were added to the mixture just prior to the final mixing zone. After extrusion, the material was quenched in a water bath at room temperature and finally pelletised. In order to investigate the effect of multiple mixings, the pelletised material was then re-fed back into the beginning of the extruder (after bleeding the extruder), and no further CNF was added. This was then repeated a third time.

After each extrusion, a small amount of the pelletised material was retained for the production of an isotropic compression-moulded sheet, and for analysis (section 3). This meant that sheets were produced from the nanocomposite material that had been mixed by a single mixing zone (after 1<sup>st</sup> extrusion), four mixing zones (2<sup>nd</sup> extrusion) and seven mixing zones (3<sup>rd</sup> extrusion). The Young's modulus of these sheets was then obtained by static tensile testing, the results of which are shown by the filled symbols (!7) in Figure 1.

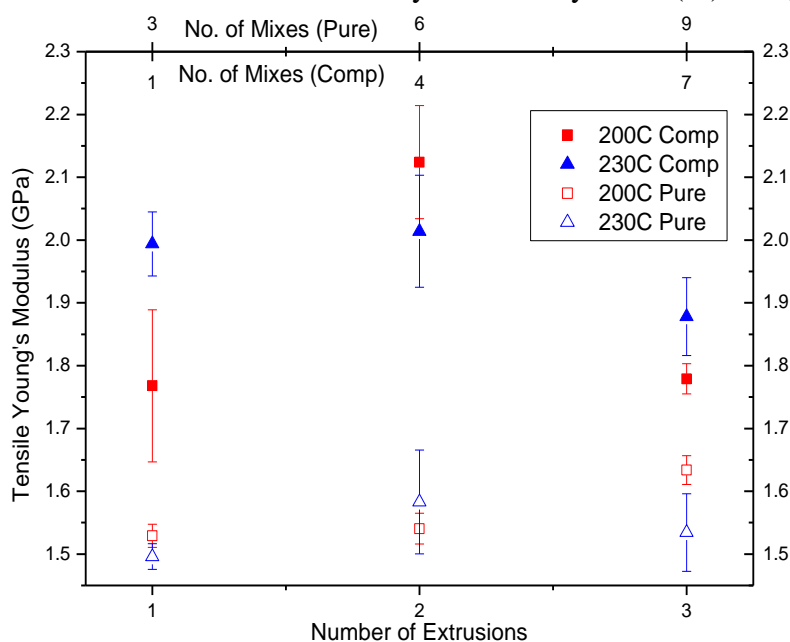


Figure 1 Young's modulus of Compression-Moulded Sheets obtained from static tensile testing. The filled symbols (!7) represent the 10% w/w Carbon Nanofibre/Polypropylene composite sheets and the open symbols (∇8) represent pure polypropylene sheets. The !∇ points were blended at 200°C and 78 points at 230°C

Figure 1 shows a clear peak in Young's modulus at (2.12±0.09)GPa, after the material had been blended by four mixing zones (2<sup>nd</sup> extrusion). The increase in Young's modulus, over the material blended by a single mixing zone, is attributed to increased dispersion of the CNF in the polypropylene matrix. The subsequent decrease in modulus in the material

blended by seven mixing zones is attributed to a shortening of the CNF due to the high shear process, which leads to a reduction in the reinforcing efficiency. This is discussed further in section 3.

Figure 1 also shows a comparison with the Young's modulus of pure polypropylene isotropic compression-moulded sheets that has been processed in an identical fashion to the composite material, the only difference being that no CNF was added during the first extrusion. This shows only a minimal variation in the Young's modulus with the number of mixtures, suggesting no degradation of the polypropylene during the blending process.

## **2.2 Melt-Spinning and Drawing to produce Oriented Tapes**

Following blending using a twin-screw extruder, the material was melt-spun into tape by passing the material through a single screw extruder, before extrusion through a collar and slot die. The extruded material was then fed onto heated rollers, with cool air blown onto the first roller to prevent overheating and solid phase drawing, and then onto a haul-off winder.

Drawing trials using a draw frame with pure polypropylene tapes showed that a nominal maximum draw ratio of 15:1 ( $15\lambda$ ) was possible before voiding became evident in the tape. It was shown that  $13\lambda$  tapes gave the best translation of properties from the drawn tapes to the hot compacted sheets. However, when the melt-spun CNF/polypropylene nanocomposite material was drawn, a nominal maximum draw ratio of only  $\sim 11.5\lambda$  could be drawn consistently.

## **2.3 Hot Compaction of drawn Oriented Tapes to produce Unidirectional Samples**

The drawn tapes were lathe wound onto a steel frame, with the pitch of the lathe set to just less than the width of the drawn tapes, typically  $\sim 1.5$ -2mm. A total of six windings were performed for each sample along the  $0^\circ$  axis, creating a total of twelve layers of tape to be compacted.

The wound samples to be compacted were placed in a mould made from a series of plates and layers, determined from previous hot compaction investigations [1-5, 10]. A thermocouple was also introduced to the surface of the sample in order to accurately register the compaction temperature. The samples were then compacted in a hydraulic press at a range of temperatures, and a contact pressure of 5MPa (700psi). The samples were compacted for a dwell time of 5 minutes from the point at which the sample reached within  $0.5^\circ\text{C}$  of the target compaction temperature, before being quenched under a contact pressure of 5MPa (700psi). When the sample temperature decreased below  $90^\circ\text{C}$  the sample was allowed to relax within the press.

These hot compacted samples were all unidirectional samples, meaning the molecular orientation in the compacted samples was oriented along the  $0^\circ$  axis only.

## **2.4 Static Tensile Testing of Hot Compacted Samples**

The Young's modulus of the hot compacted sheets (and compression moulded sheets in Figure 1) was taken from the initial linear region (small strain) of stress/strain curves measured using a servo-mechanical testing machine at a room temperature of  $21 \pm 1^\circ\text{C}$ . The tensile tests were performed on dumbbell-shaped specimens (total size of  $75 \times 12.3\text{mm}$ , with the narrower testing portion of the dumbbell measuring  $\sim 27 \times 4\text{mm}$ ). A nominal strain rate of  $5 \times 10^{-3} \text{ s}^{-1}$  was used for all tests, with a small pre-load applied ( $\sim 2$ -5N) in order to ensure that the linear region of the stress/strain curve was preserved and not affected by effects due to straightening within the testing area. The sample strain was measured using a video extensometer to track black/white boundary targets ( $\sim 20\text{mm}$  apart) and marked across the width of the target area of the sample. Preliminary results in Figure 2 show the variation in Young's modulus with increasing compaction temperature for pure polypropylene and nanocomposite polypropylene/CNF hot compacted samples.

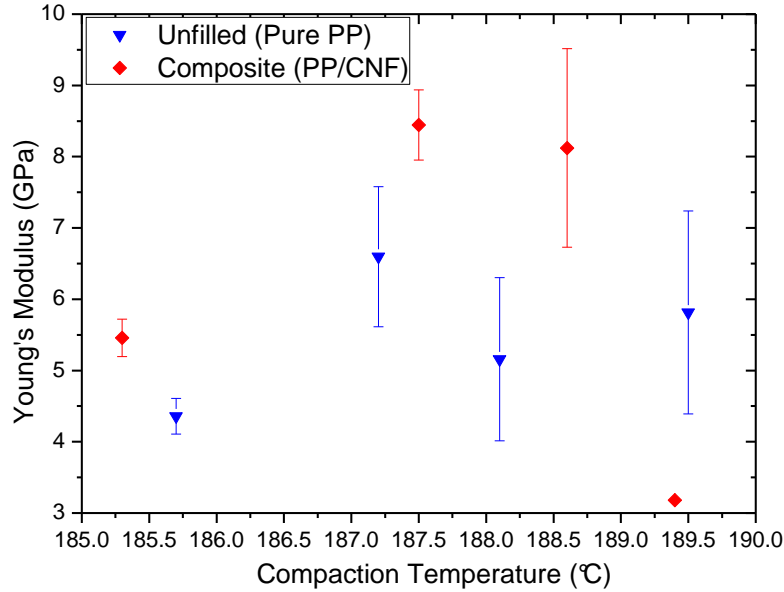


Figure 2 Young's modulus of Hot Compacted Samples for a number of samples compacted in the range 185-190°C, for tapes drawn to 11.5λ. The blue points (B) are the pure polypropylene samples and red points (A) correspond to the filled composite samples.

The optimum compaction temperature is defined as the compaction temperature at which the Young's modulus is at a maximum value. This is clearly visible in Figure 2 for the composite samples (optimum compaction temperature of ~188°C); although the optimum compaction temperature is not as clear for the pure polypropylene compacted samples. Previous tests with pure polypropylene hot compacted samples have shown a much more clearly defined peak than that seen in Figure 2, and along with visual inspection of the samples, indicate that the optimum compaction temperature should also be ~188°C.

Figure 2 also shows that, as with the isotropic sheets in Figure 1, the stiffness of the hot compacted sheets is also increased due to the incorporation of the carbon nanofibres. The optimally compacted pure polypropylene sample in Figure 2 had a Young's modulus of  $(6.60 \pm 0.98)$  GPa, and the corresponding optimally compacted composite sample had a modulus of  $(8.45 \pm 0.49)$  GPa, an increase of 28%. Similarly there was a 22% increase in the failure stress of the sample, from  $(203 \pm 47)$  MPa to  $(248 \pm 22)$  MPa. The strain at this maximum stress decreased 25% from  $(9.71 \pm 0.38)\%$  for the pure hot compacted samples to  $(7.37 \pm 0.67)\%$  for the filled nanocomposite compacted samples.

The hot compacted sheets show properties comparable with those seen in a similar study [10], although in the previous work the effect of reinforcement from the incorporation of the CNF was not so pronounced.

### 3. Modelling and Analysis

A key part of this project is to link the structure of the composite samples produced to their properties. In order to do this, a variety of techniques have been employed to understand the effect of the various processing steps upon the material. The most important of these have been to attempt to measure the dimensions of the CNFs both prior to, and at various stages of, the blending process.

#### 3.1 Scanning Electron Microscopy (SEM) Image Analysis

Polypropylene/CNF pellets that were removed from the blending process after each extrusion, as described in section 2.1, were placed into a furnace at 400°C for two hours,

burning off the polypropylene matrix and leaving a CNF residue. The CNF were then dispersed in a water/surfactant solution and placed onto an SEM stub, as was a sample of the as-received CNF. All sample SEM stubs were sputter-coated with platinum in argon plasma before observation.

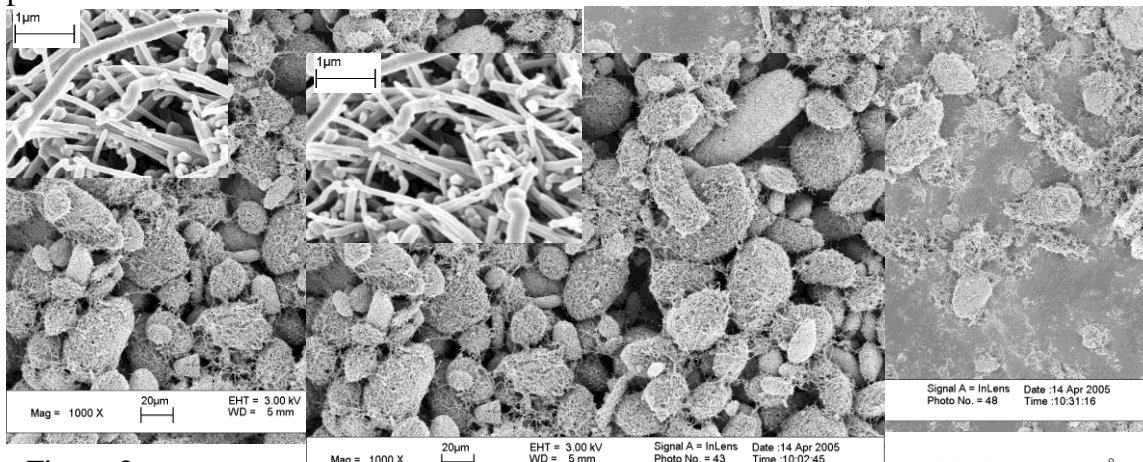


Figure 3. SEM image of as-received CNFs. The size of the balls proved to be a good indication of the extrusion process (one mixing zone). Although how the extrusion process broke up the CNF is a good indication of the assembly. The scale bar indicates 20µm. The majority have begun to be broken up. The scale inset shows a higher magnification of the CNF. The scale bar indicates 20µm.

Figure 3 shows the as-received CNFs and the highly entangled ‘balls’ that they form. The inset of Figure 3 also shows a number of the different forms of the individual fibres, which include variation in length, diameter and the degree of linearity. Both straight-sided fibres and ‘bamboo’ type structures can also be seen, as have been reported elsewhere [10].

After a single extrusion (one mixing zone) the CNF ‘balls’ seen in Figure 3 were not completely broken up, and there were a number of large clumps still visible. This can be seen in Figure 4. However there were also a number of individual fibres present, indicating that the high-shear process in the twin-screw is able to remove fibres from the ‘balls.’

When the polypropylene was burned off from pellets from further extrusions (further mixing), neither the highly entangled ‘ball-like’ structures nor many individual fibres were visible. Instead large ‘mat’-like structures much larger than the ‘balls’ were seen, attributed to re-aggregation of the CNF on the surface of a bubble, formed as the polypropylene was vaporised.

### 3.2 Diameter Measurements

Although the length of the CNF could not be measured directly from the SEM images due to high entanglement of the fibres, it was possible to measure the diameter. Using an image analysis program the average diameter of each fibre on a number of SEM images was determined. A total of 220 fibres were measured, for which the distribution of fibre diameters is shown in Figure 5. This distribution gives an average diameter of  $(92.8 \pm 2.6) \text{ nm}$ , which is consistent with other measurements made in the literature [9, 10].

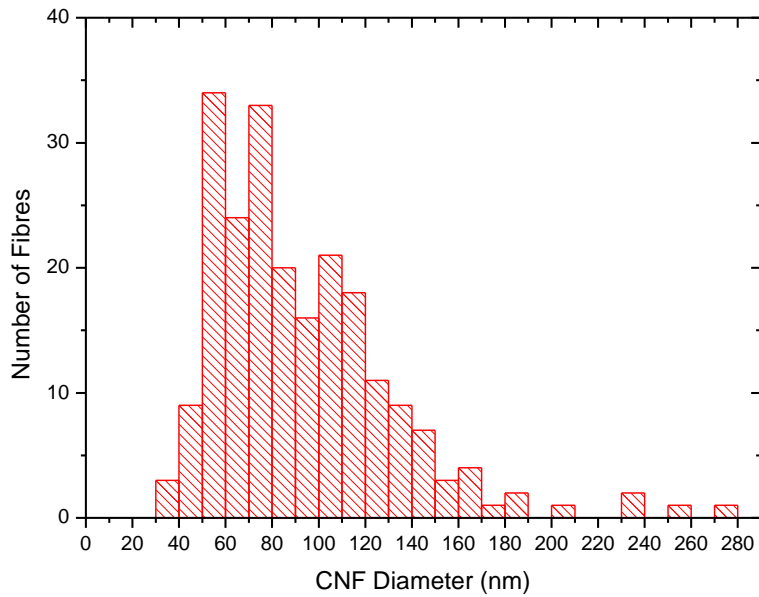


Figure 5 Distribution of CNF Diameter measured using Image Analysis on SEM images. A total of 220 fibres were measured, giving an average diameter of 92.8nm and standard error of 2.6nm.

### 3.3 Dynamic Light Scattering (DLS)

Because SEM image analysis proved inconclusive in measuring the length of the CNF pre- and post-blending, it was necessary to use alternative methods to measure this critical quantity. DLS works by measuring the real-time fluctuations in the scattered light from a sample, due to the diffusion of the scattering centres through the solution. Usually these scattering centres are spherical particles, however recent work has extended this technique to macromolecules [11], and rod-like particles [12].

Preliminary results with this technique have been promising. Following the method in [12], a solution of  $\sim 2 \times 10^{-3}$  % w/w CNF was prepared, using a hot filtration method to remove the CNF from the nanocomposite pellets. The analysis from [12] was then fitted to the data, as shown in Figure 6.

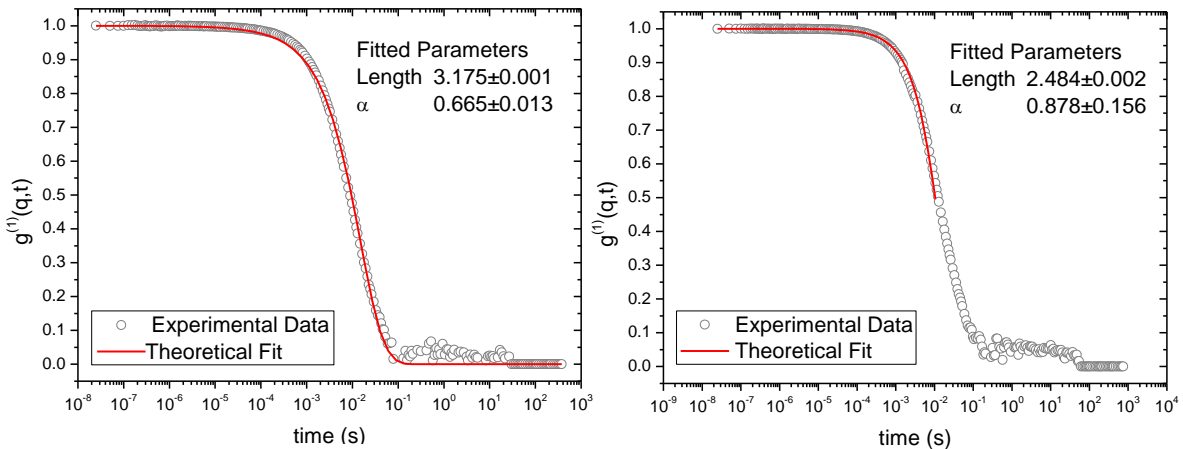


Figure 6 Autocorrelation scattering functions from DLS. Both show scattering at  $30^\circ$ . The left-hand pane is scattering from CNF mixed by four mixing zones, the fit giving a CNF average length of  $(3.175 \pm 0.001) \mu\text{m}$ . The right-hand pane is scattering from CNF mixed by seven mixing zones, with an average length of  $(2.484 \pm 0.002) \mu\text{m}$ . CNF diameter in both cases was fixed at 92.8nm, from image analysis in section 3.2.  $\alpha$  describes the distribution of lengths, where  $\alpha=1$  for a monodisperse distribution.

Figure 6 confirms that there is a reduction in length of the CNFs with an increasing number of mixes, confirming the explanation given in 2.1 to explain the reduction in Young's

modulus in Figure 1. Because the diameter of the fibres should not change with the amount of mixing, the aspect ratio of the fibres is decreased from 34 to 27, and as can be seen in 3.4, this reduces the efficiency of reinforcement. The fitting also includes a parameter,  $\alpha$ , describing the spread of the distribution of lengths, and the results suggest the distribution becomes narrower as the number of mixes increases. No scattering is included for CNF blended by one mixing zone, because this single mix does not disentangle the CNF and so scattering cannot be attained from individual fibres.

### 3.4 Cox-Krenchel Modelling

First attempts at modelling have followed the simple rule of mixtures approach. The Cox-Krenchel model is a modification of Cox's 1952 "shear-lag" analysis of an elastic fibre embedded in an elastic matrix, to take into account partially oriented composites using Krenchel's 1964 analysis [13]. The composite modulus is thus given by:

$$E_c = \eta_o \eta_l V_f E_f + (1 - V_f) E_m$$

Where  $E_c$  is the composite modulus,  $V_f$  is the fibre volume fraction,  $E_f$  is the fibre modulus,  $E_m$  is the matrix modulus, and  $\eta_o$  and  $\eta_l$  are the orientation and length efficiency factors. A value of 240GPa was taken from the literature for the CNF modulus [9], the polypropylene matrix was measured from an isotropic sample to be  $(1.61 \pm 0.03)$ GPa, and the fibre volume fraction was fixed to be 5% v/v (10% w/w). In addition it was necessary to estimate Poisson's ratio to be 0.35, such that  $\eta_l$  could be calculated. For further details on calculating  $\eta_l$  and  $\eta_o$ , and the "shear-lag" analysis, see ref [13]. The Young's modulus of the composite material can be calculated as a function of the fibre aspect ratio, as shown in Figure 7.

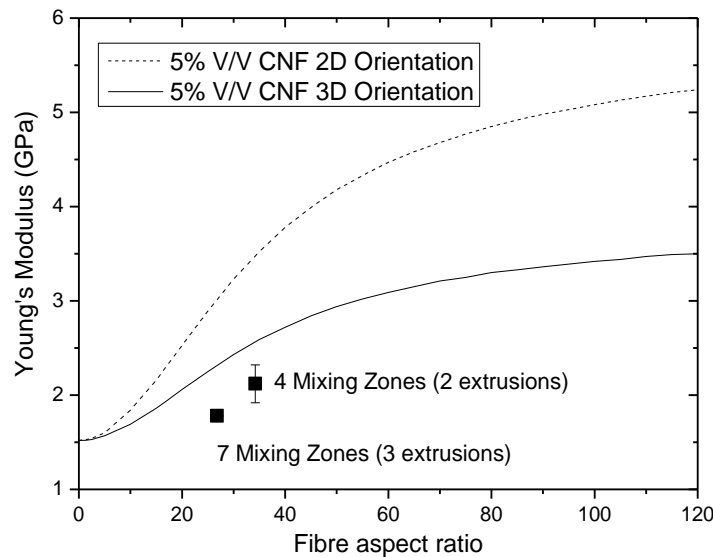


Figure 7 Predicted Composite Young's Modulus as a function of the fibre aspect ratio, modelled for randomly oriented fibres, within two degrees of freedom ( $\square$ ) and three degrees of freedom ( $\square$ ) at 5% v/v CNF. The datapoints (!) indicate the experimentally measured composite values of modulus and the fibre aspect ratio from SEM and DLS measurements.

Figure 7 shows Young's modulus predictions for two model orientation states (2D and 3D) as a function of the fibre aspect ratio (5% v/v). It can be seen that the Young's modulus of a CNF/polypropylene isotropic sheet was predicted to increase quite sharply initially with increasing aspect ratio of the fibre reinforcement phase, and begins to flatten off above an aspect ratio of  $\sim 60$ . Also shown are two experimental datapoints, the Young's modulus from the compression-moulded sheets in Figure 1. The fibre aspect ratio was taken from the DLS and SEM image analysis results described above.

Although the experimental data does not fit the theoretical predictions, there are a number of possible reasons for this. Firstly, using DLS to measure the length of the fibres is a new

technique, and has yet to be refined. Secondly, SEM images show a thin (~10nm) trans-crystalline region, consisting of row crystallised chains nucleated on the CNF when embedded in the polypropylene matrix. This region will exhibit different mechanical properties to the bulk matrix, and is not taken into account in the current model. Thirdly, Figure 3 shows that the CNF are not straight, which is also observed when the fibres are embedded in the matrix. The model described above assumes straight fibres reinforcing the matrix, and so will be overestimating the composite modulus.

#### 4. Conclusions

Blending of vapour-grown carbon nanofibres into polypropylene at a loading of 10% w/w has been achieved by twin-screw extrusion. Compression-moulded isotropic sheets produced have shown an increase in mechanical properties over pure polypropylene sheets. Hot compaction of the composite material has also proved successful, showing a 28% increase in Young's modulus over hot compacted pure polypropylene at optimum compaction conditions.

The key finding to date, has been the use of dynamic light scattering and image analysis to measure the aspect ratio of the CNF, and how this varies during the blending process. This had not been achieved previously.

Modelling to link the composite structure and properties is still at an early stage of development, although it is becoming clear that a simple two phase model, such as the Cox-Krenchel model, may not be sufficient to describe these types of composites.

#### Acknowledgements

We thank the University of Leeds Nanomanufacturing Institute (NMI) for funding this research. We would also like to thank Manlio Tassieri and Dr Tom Waigh for their help and expertise with Dynamic Light Scattering, Dr Simon J Antony for his collaboration and Dr Mark Bonner for his assistance.

#### References

1. **Hine, P. J., et al.**, "Hot compaction of high modulus melt-spun polyethylene fibres", *Journal of Materials Science*, **28/2**, (1993), 316-324.
2. **Hine, P. J., et al.**, "A comparison of the hot-compaction behaviour of oriented, high-modulus, polyethylene fibres and tapes", *Journal of Macromolecular Science - Physics*, **40 B/5**, (2001), 959-989.
3. **Ward, I. M., Hine, P. J.**, "The science and technology of hot compaction", *Polymer*, **45/5**, (2004), 1423-1437.
4. **Hine, P. J., Ward, I. M., Teckoe, J.**, "The hot compaction of woven polypropylene tapes", *Journal of Materials Science*, **33/11**, (1998), 2725-33.
5. **Hine, P. J., et al.**, "The hot compaction behaviour of woven oriented polypropylene fibres and tapes. I. Mechanical properties", *Polymer*, **44/4**, (2003), 1117-31.
6. **Gordeyev, S. A., et al.**, "A promising conductive material: highly oriented polypropylene filled with short vapour-grown carbon fibres", *Materials Letters*, **51/1**, (2001), 32-6.
7. **Kuriger, R. J., et al.**, "Processing and characterization of aligned vapor grown carbon fiber reinforced polypropylene", *Composites Part A (Applied Science and Manufacturing)*, **32A/1**, (2002), 53-62.
8. **Kuriger, R. J., Khairul Alam, M.**, "Extrusion conditions and properties of vapor grown carbon fiber reinforced polypropylene", *Polymer Composites*, **22/5**, (2001), 604-612.
9. **Tibbetts, G. G., McHugh, J. J.**, "Mechanical properties of vapor-grown carbon fiber composites with thermoplastic matrices", *Journal of Materials Research*, **14/7**, (1999), 2871-80.
10. **Hine, P., Broome, V., Ward, I.**, "The incorporation of carbon nanofibres to enhance the properties of self reinforced, single polymer composites", *Polymer*, **46/24**, (2005), 10936-10944.
11. **Carrick, L., et al.**, "The internal dynamic modes of charged self-assembled peptide fibrils", *Langmuir*, **21/9**, (2005), 3733-3737.
12. **Badaire, S., et al.**, "In situ measurements of nanotube dimensions in suspensions by depolarized dynamic light scattering", *Langmuir*, **20/24**, (2004), 10367-10370.
13. **Folkes, M. J.**, "Short Fibre Reinforced Thermoplastics". 1985, Chichester, New York, Brisbane, Toronto, Singapore:Research Studies Press, Division of John Wiley & Sons.